Ioffe Institute
6th Int. Symp. "Nanostructures: Physics and Technology"
St Petersburg, Russia, June 22–26, 1998.

GaN-based two-dimensional electron devices

M. S. Shur and R. Gaska†
Rensselaer Polytechnic Institute, Troy, NY 12180-3590, shurm@rpi.edu
† APA Optics, Inc., 2950 N. E., 84th Lane, Blaine, MN 55449

Abstract. We discuss the properties of the two dimensional (2D) electron gas at AlGaN/GaN heterointerface. The density of the 2D gas is affected by piezoelectric effects and by doping levels in both AlGaN and GaN layers. The record values of the sheet carrier density have been achieved with sheet electron densities of the two-dimensional electron gas on the order of $1.5 \times 10^{13}\,cm^{-2}$ and the sheet carrier concentration in the surface heterostructure channel as high as $4 \times 10^{13}\,cm^{-2}$. At high electron concentration, electrons are divided between the 2D and 3D states, and this division affects the electron mobility in the channel. Optical polar scattering, impurity scattering, and piezoelectric scattering limit the mobility. The largest electron mobility was observed in AlGaN/GaN heterostructures grown on SiC. At room temperature, the mobility is over 2,000 cm^2/V-s; at cryogenic temperatures, the highest mobility is over 10,000 cm^2/V-s. These values are high enough for the observation of the Quantum Hall Effect. Multichannel 2D electron structures are being developed that will allow us to achieve a much higher current density and much higher power.

1 Introduction

The first evidence of the existence of the two-dimensional electron gas at the GaN/AlGaN heterointerface was provided by a large mobility enhancement at the heterointerface. In 1995, Khan et al. [1] observed a large mobility enhancement in the 2D-electron gas at the AlGaN/GaN interface. They measured the 2D electron gas Hall mobility around 5,000 cm^2/V-s at 80 K, compared to the maximum electron mobility of approximately 1,200 cm^2/V-s in their bulk doped GaN samples. Recently, Gaska et al. [2] reported on the electron mobility in the 2D-gas electron gas at the GaN/AlGaN interface exceeding 10,000 cm^2/V-s at cryogenic temperatures and exceeding 2000 cm^2/V-s at room temperature. These values were observed in the samples with very high sheet carrier concentration (on the order of $10^{13}\,cm^{-2}$).

Our estimates show that the maximum density of the two-dimensional electron gas at the GaN/AlGaN heterointerface or in GaN/AlGaN quantum well structures can reach $5 \times 10^{13}\,cm^{-2}$, which is more than an order of magnitude higher than for traditional GaAs/AlGaAs heterostructures. The mobility-sheet carrier concentration product for these two dimensional systems might also exceed that for GaAs/AlGaAs heterostructures and can be further enhanced by doping the conducting channels and by using "piezoelectric" doping [3, 4], which takes advantage of high piezoelectric constants of GaN and related materials.

The University of California, Santa Barbara group [5] reported record-breaking microwave power close to 3 W/mm achieved in GaN-based Heterostructure Field Effect Transistors. Their results (and similar, though not as spectacular results achieved by other groups [6]) show that these devices will compete with GaAs-based transistors in high power, high frequency applications.

In this paper, we review our recent results obtained for AlGaN/GaN heterostructures. We discuss the properties of the 2D-electron gas at AlGaN/GaN heterointerface with emphasis on the differences between these structures and their GaAs counterparts.

2 Band structure

Fig. 1 (from [7]) shows a typical band diagram of an AlGaN/GaN heterostructure. Notice the difference in the electric field slopes in GaN and AlGaN at the heterointerface. This difference is related to piezoelectric effect, and this band diagram is very different from a band diagram for a typical AlGaAs/GaAs heterostructure.

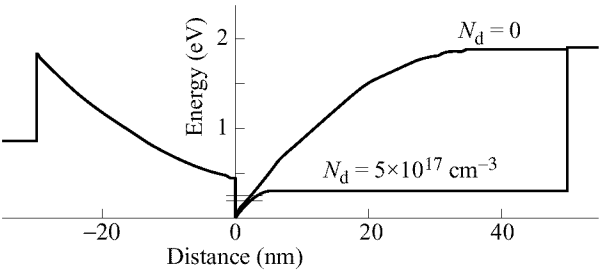

Fig 1. Band diagrams of the GaN heterostructures for doped and undoped GaN layers. The short horizontal lines show the position of the Fermi level (top line) and of the lowest subband (bottom line). Al mole fraction is $x = 0.2$. Schottky barrier height is 1 eV. Conduction band discontinuity, $\Delta E_c = 0.75\Delta E_g$. AlGaN doping, $5 \times 10^{18}\,\mathrm{cm}^{-3}$. 2D gas density is $5 \times 10^{12}\,\mathrm{cm}^{-2}$. $T = 300$. The electron effective mass is $0.23m_0$. The piezoelectric constants are $e_{31} = -0.58\,\mathrm{C/m}^2$, $e_{33} = 1.55\,\mathrm{C/m}^2$; $e_{31} = -0.36\,\mathrm{C/m}^2$, $e_{33} = 1\,\mathrm{C/m}^2$, for AlN and GaN, respectively. Material parameters of AlGaN were determined by taking a linear interpolation between GaN and AlN parameters as functions of the Al molar fraction. (From [7].)

Fig. 2 shows the position of the Fermi level, E_F, (counted from the bottom of the conduction band in GaN at the heterointerface) as a function of the sheet electron density, n_s [7]. Also shown the Al molar fraction, which corresponds to the value of the conduction band discontinuity at the heterointerface. The effective mass of $0.24m_e$ (where m_e is the free electron mass) was assumed in this calculation. The first seven subbands were accounted for. For n_s higher than $1.5 \times 10^{12}\,\mathrm{cm}^{-2}$, the following approximation:

$$E_F = E_0 + n_s/D \tag{1}$$

is in good agreement with the computed dependence.

Fig. 2 shows that the values of n_s close to $2 \times 10^{13}\,\mathrm{cm}^{-2}$ can be achieved for relatively low Al molar fractions. Such high concentrations are not achievable in AlGaAs/GaAs or even in AlInAs/InGaAs, which has a larger conduction band discontinuity than AlGaAs. Much higher values of n_s in the AlGaN/GaN heterostructures can be achieved by doping the active layer so the total surface electron concentration in the channel

$$N_s = n_s + N_d d \tag{2}$$

This increase is related to the change in the band diagram caused by the channel doping illustrated by Fig. 1. As seen from Fig. 1, in the doped quantum well structures,

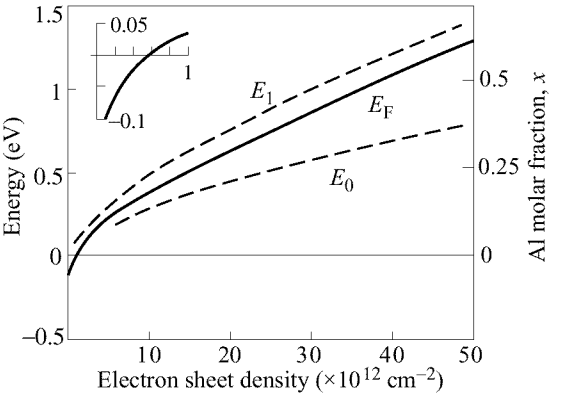

Fig 2. Fermi level (solid line) and the positions of the ground and first excited subbands for GaN/AlGaN heterostructure counted from the bottom of the conduction band in GaN at the heterointerface. The insert shows the position of the Fermi level at small values of n_s. Also shown the Al molar fraction, with corresponds to the value the conduction band discontinuity equal to the energy scale on the left [7].

electrons can go into bulk states, whose density is large enough to contain a very large electron sheet density.

Another important approach in increasing the electron sheet concentration, which is important for applications in power devices, is to use multichannel structures that have several parallel 2D-electron gas layers. Gaska et al. [8] report on the fabrication, characterization, and modeling of a double channel $Al_xGa_{1-x}N$/GaN Heterostructure Field Effect Transistors. The epilayer structure was grown by low pressure Metal Organic Vapor Pressure Epitaxy on sapphire substrates. In these structures, a 50 nm AlN layer growth on sapphire was followed by the deposition of a 0.8 μm nominally undoped GaN layer, 25 nm of $Al_{0.25}Ga_{0.75}N$, a second 0.1 μm nominally undoped GaN layer, and finally capped with 30 nm $Al_{0.25}Ga_{0.75}N$ barrier layer (see Fig. 3). Both AlGaN barrier layers were unintentionally doped with electron concentration of approximately $n = 10^{18}$ cm^{-3}. Devices with the source-drain spacing of 5 μm, the gate length of 2 μm and the gate width of 50 μm were fabricated. Ti/Al/Ti/Au of thickness 250/700/500/1000 angstroms was annealed at 900°C for 30 sec to make ohmic contacts; Pt/Au was used for the offset gate fabrication. The maximum source-drain current at zero gate bias was 0.5 A/mm, the maximum transconductance $g_m = 140$ mS/mm was measured at the gate bias of -1.5 V. The threshold voltage of these devices was -4.5 V.

Fig. 4 shows a qualitative band diagram of such a structure. The 25 nm AlGaN layer sandwiched between two GaN layers formed a Semiconductor-Insulator-Semiconductor structure. As was shown in [3, 9], strong piezoelectric effects cause the depletion at the top interface of this structure and accumulation at the bottom interface. This accumulation layer creates the second conducting channel in our devices. This conducting channel is separated from the ohmic source and drain contacts by the depleted region in GaN and by the thin AlGaN layer. Hence, this bottom conducting has very large series resistances at low drain biases. At high drain biases, the electron injection drastically decreases the series resistances for the bottom channel, and it starts contributing to the

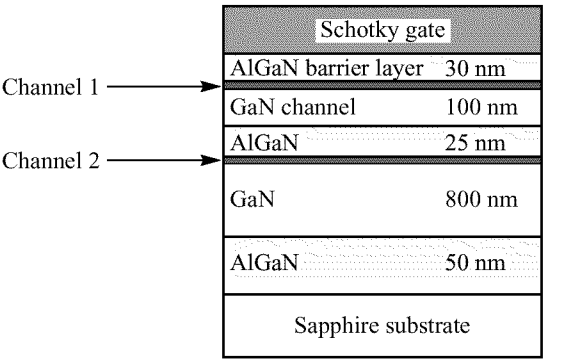

Fig 3. AlGaN/GaN epitaxial structure with two channels (after [8]).

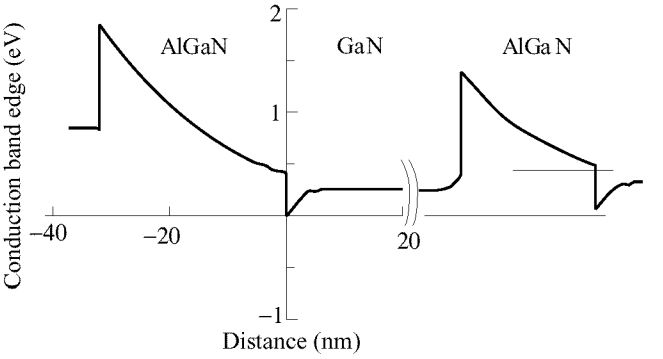

Fig 4. Qualitative band diagarm of two channel AlGaN/GaN heterostructure.

overall drain current. This contribution is responsible for a characteristic kink in the output characteristics at high drain biases.

Gaska et al. [8] also developed an analytical device model for a double channel HFET based on the Unified Charge Control Model. The model describes both subthreshold and above threshold regimes of operation and accounts for the drain-bias dependent series resistances for the bottom channel and accurately reproduces the measured current-voltage characteristics. The modeling results showed that such improved multichannel AlGaN-GaN heterostructures will be very promising for applications in power GaN-based HFETs.

The band diagrams shown above assume an abrupt AlGaN/GaN heterointerface. However, recent experimental and theoretical studies of the capacitance-voltage (C–V) characteristics and of the Hall mobility of the 2D-electron gas for strained $Al_{0.25}Ga_{0.75}N$-GaN heterostructures showed that the heterointerface might be graded. The heterostructures studied in [10] were grown on sapphire with the AlGaN barrier layer thickness varying from 10 nm to 100 nm. The measured C–V characteristics provided the strong experimental evidence that the piezoelectric effect causes an increase in the sheet electron concentration in heterostructures with $Al_{0.25}Ga_{0.75}N$ thickness up to 60 nm.

The strain-induced electric field changes the charge distribution in the heterostruc-

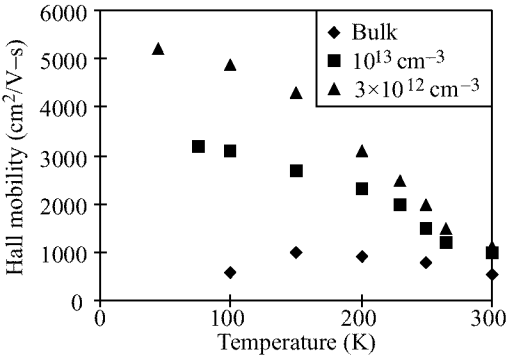

Fig 5. Hall 2D-electron gas mobility in bulk GaN and nominally undoped ($n_s = 3 \times 10^{12}\,cm^{-3}$) and doped ($n_s = 10^{13}\,cm^{-3}$) AlGaN/GaN heterostructures versus temperature [13].

tures. This, in turn, caused the shift of the C–V characteristics with respect to their unstrained positions while preserving their general shape. The magnitude of the shift depends on the strain and the strained layer thickness. The magnitude of strain was extracted from the comparison between the calculated and measured C–V characteristics. The results showed that relaxation increased gradually with the AlGaN thickness. The structure with a 100-nm thick barrier layer was fully relaxed. The conventional theory of strain relaxation for abrupt interfaces yields the critical thickness of unrelaxed $Al_{0.25}Ga_{0.75}N$ barrier at least 1.5 times smaller than the value extracted from these C–V measurements. In Reference [10], this difference was attributed to a gradual change in the Al mole fraction near the AlGaN-GaN heterointerface over approximately 5–6 nm.

3 Transport properties

A high electron sheet density in AlGaN/GaN heterostructures is very effective in screening the impurity scattering [11]. Recent measurements of the Quantum Hall and Shubnikov–de-Haas effect on similar AlGaN-GaN modulation doped structures with Si-doped channels clearly showed the existence of the two-dimensional (2D) electron gas in these structures with parallel conduction path provided by three-dimensional electrons [12]. The Hall mobility measurements and theoretical calculations reported in [11] showed that the 2D-electron gas mobility in doped channel structures at room temperature is nearly the same as in undoped structures. This is confirmed by our more detailed measurements shown in Fig. 5 [13].

Recent measurements of the Hall mobility and Quantum Hall Effect in the AlGaN/GaN HFETs grown on SiC substrates showed the electron mobility in these structures in considerably large than in similar structure grown on sapphire substrates, especially at cryogenic temperatures [2, 12]. This can be explained by a better material quality of GaN grown on SiC substrates because of much smaller lattice mismatch between AlGaN and SiC. A better material quality may manifest itself in a smaller dislocation density and/or in a less pronounced columnar structure. The dislocation density in GaN grown on sapphire is quite high (in the range $10^8 - 10^{10}\,cm^{-2}$ [14].) This material also has a pronounced columnar structure (called ordered polycrystalline microstructure [12].) The mobility limited by the dislocations is roughly proportional to

temperature [13]. The polycrystalline structure leads to the observation of the "mobility edge" [15] and may result in the exponential temperature dependence of the mobility with a very small, concentration-dependent activation energy [16]. Both scattering mechanisms related to the material imperfections should be much more pronounced at cryogenic temperatures. Hence, the data reported in [2] point out to a better material quality of GaN grown on SiC substrates.

Further studies [17] showed that at high electron densities, electrons occupy three-dimensional states in the doped channel near the GaN-AlGaN heterointerface, even at moderate doping levels, on the order of $10^{17}\,cm^{-3}$. This model explains the observed decrease of room temperature electron Hall mobility with the channel doping. The mobility in $Al_{0.2}Ga_{0.8}N$-GaN heterostructures grown on sapphire and conducting 6H–SiC substrates decreases from 1,200 cm^2/Vs (on sapphire) and 2,000 cm^2/Vs (on 6H–SiC) at electron sheet density $n_s = 10^{13}\,cm^{-2}$, to approximately 700–800 cm^2/Vs at $n_s > 3 \times 10^{13}\,cm^{-2}$ for both types of the substrates. The model also explains a non-monotonous electron mobility dependence on the gate bias in the "gated" Hall slab at temperature $T = 4.2$ K. The measured Hall mobility at 4.2 K first increases with the gate bias (from approximately 7,000 cm^2/V-s at $V_g = -4$ V up to the record value of 11,000 cm^2/V-s at $V_g = -0.5$ V). With a further increase in V_g, the mobility decreases down to 9,500 cm^2/V-s at $V_g = 1.5$ V). With an increase in the gate bias from -4 V to 1.5 V, the sheet electron carrier concentration increases from approximately $3.5 \times 10^{12}\,cm^{-2}$ to $1.1 \times 10^{13}\,cm^{-3}$. At the gate bias -0.5 V, which corresponds to the maximum Hall mobility, the electron sheet concentration is $8 \times 10^{12}\,cm^{-2}$ and is close to the maximum value of n_s estimated for the 2D channel near $Al_{0.2}Ga_{0.8}N$-GaN heterointerface.

These results are important for choosing the optimum doping in AlGaN-GaN Doped Channel Heterostructure FETs, which should be dependent on the gate length.

Acknowledgment

I would like to thank my colleagues Drs. Bykhovski, Gelmont, Kaminski, Chen, Khan, Yang, Soloviov, Osinsky, Fjeldly, Knap, Contreras, Alause, Skiberbiszewski, Professors Camassel, Dyakonov, Robert, Dr. Sadowski, Huant, F. J. Yang, Goiran, and J. Leotin, who contributed to the research described in this paper. The work at Rensselaer Polytechnic Institute and at APA Optics has been supported by the Office of Naval Research and by the Cornell University (under the MURI subcontract).

References

[1] M. A. Khan, Q. Chen, C. J. Sun, M. S. Shur, and B. L. Gelmont, *Appl. Phys. Lett.* **67** No. 10, Sep. 4, 1429–1431 (1995).

[2] R. Gaska, J. W. Yang, A. Osinsky, Q. Chen, M. Asif Khan, A. O. Orlov, G. L. Snider, and M. S. Shur, *Appl. Phys. Lett.* **72** No. 6, 707–709, Feb. 1998.

[3] A. Bykhovski, B. Gelmont, and M. S. Shur, *J. Appl. Phys.* Dec. **74** (11), 6734 (1993).

[4] P. M. Asbeck, G. J. Sullivan, E. T. Yu, S. S. Lau, and B. McDermott, *Device Research Conference Abstracts*, paper V-B-5, Fort Collins, Colorado (1997).

[5] B. J. Thibeault, B. P. Keller, Y.-F. Wu, P. Fini, U. K. Mishra, C. Nguyen, N. X. Nguyen, and M. Le, *IEDM-97 Technical Digest*, IEEE, December (1997).

[6] Q. Chen, R. Gaska, M. Asif Khan, Michael S. Shur, G. J. Sullivan, A. L. Saylor, and J. A. Higgins, *IEEE Electron Device Lett.* **19** No. 2, 44–46, Feb. (1998).

[7] M. S. Shur, *Symposium Proc. of Material Research Society*, Symposium E, Fall 1997, (to be published).
[8] R. Gaska, M. S. Shur, J. Yang, and T. A. Fjeldly, *MRS, Symposium D*, Spring, accepted (1998).
[9] A. D. Bykhovski, B. Gelmont, and M. S. Shur, *J. Appl. Phys.* **78** (6), 3691–3696, 15 September (1995).
[10] A. D. Bykhovski, R. Gaska, J. W. Yang, and M. S. Shur, submitted to *Electronic Materials Conference*, June 1998, Charlottesville, VA.
[11] M. S. Shur, B. Gelmont, and M. Asif Khan, *J. Electronic Materials* **25** No. 5, 777–785, May (1996).
[12] W. Knap, S. Contreras, H. Alause, C. Skiberbiszewski, J. Camassel, M. Dyakonov, J. L. Robert, J. Yang, Q. Chen, M. Asif Khan, M. Sadowski, S. Huant, F. J. Yang, M. Goiran, J. Leotin, and M. Shur, *Appl. Phys. Lett.* **70** (16), 2123–2125 (April (1997).
[13] M. S. Shur, Q. Chen, J. Yang, R. Gaska, M. Blasingame, M. Asif Khan, A. Ping, I. Idesida, V. P. Madangarli, and T. S. Sudarshan, *Proceedings of ISDRS-97*, pp. 377–380, Charlottesville, VA, Dec. (1997).
[14] S. D. Hersee, J. C. Ramer, and K. J. Malloy, *MRS Bulletin* **22** No. 7, 45–51, July (1996).
[15] B. P. Pödör, *Phys. status solidi*, **16**, K167 (1966); B. Heying, X. H. Wu, S. Keller, Y. Li, D. Kapolnek, B. P. Keller, S. P. Denbaars, and J. S. Speck, *Appl. Phys. Lett.* **68** 643 (1996).
[16] C. H. Seager, *Ann. Rev. Mater. Sci.* **15** 271 (1985).
[17] R. Gaska, J. W. Yang, M. S. Shur, A. O. Orlov, and G. L. Snider submitted to *Electronic Materials Conference*, June 1998, Charlottesville, VA.